DELPHI Collaboration

DELPHI 2001-016 CONF 457
7 March, 2001

A Measurement of the Cross Section Ratio R_b and the Forward-Backward Asymmetry A_{FB}^b for $b\bar{b}$ Events with the DELPHI Detector at LEP 2.

E. Brodet, P. Brückman[1], P. Collins, M. Elsing, T. Lesiak[1], W. Liebig, G.Wilkinson

Preliminary

Abstract

Measurements of the cross section ratio $R_b = \sigma_{b\bar{b}}/\sigma_{\mathsf{had}}$ and the b quark forward-backward asymmetry A_{FB}^b have been performed in $e^+e^- \to Z/\gamma^*$ events with the DELPHI detector using data delivered by LEP from 1997 to 2000. They correspond to centre-of-mass energies ranging from 183 to 209 GeV and comprise a total integrated luminosity of $650\,\mathrm{pb}^{-1}$. For the identification of $b\bar{b}$ events a tagging variable was used which combines the information coming from B lifetime, the mass found in secondary vertices and the rapidity of tracks coming from a secondary vertex.

The asymmetry measurement uses the charged tracks to distinguish between the b and $\overline{b}$ hemispheres. A_{FB}^b is extracted from the charge signed polar angle distribution using an unbinned log likelihood fit.

Prepared for winter conferences 2001

[1]partially supported by the KBN grant 2 P03B 111 16 and SPUB-M/CERN/P-03/DZ 297/2000

1 Introduction

During the last five years the LEP accelerator has delivered nearly $700\,\mathrm{pb}^{-1}$ to each of the four experiments at centre-of-mass energies ranging from 130 to 209 GeV. In this energy region above the Z resonance the photon exchange and its interference with the Z is no longer suppressed with respect to the Z exchange, resulting in a very different behaviour of the production characteristics of fermion pair events.

A measurement of the cross section ratio R_b and the forward-backward asymmetry A^b_{FB} has been performed at energies between 183 and 209 GeV using data collected with the DELPHI detector [1]. Unlike at LEP 1, R_b is defined as $\frac{\sigma_{b\bar{b}}}{\sigma_{\mathsf{had}}}$ rather than $\frac{\Gamma(Z\to b\bar{b})}{\Gamma(Z\to \mathrm{had})}$. The $b\bar{b}$ events are isolated using well understood techniques developed at LEP1, with efficient b tagging extended to a polar angle of 25° due to the LEP 2 silicon tracker upgrade. The b tagging is cross calibrated using data taken on the Z resonance in the same running periods as the high energy data. The good efficiency, together with the large amount of data accumulated, allows a test of the Standard Model prediction for $b\bar{b}$ production in two-fermion events. Previous results concerning the energy range 130–172 GeV can be found in ref. [2].

The paper starts with the presentation of the selection and b tagging techniques applicable to both the R_b and A^b_{FB} measurements, followed by a separate description of the measurements themselves.

2 Track Selection

The polar acceptance for charged tracks is limited by the geometry of the tracking system to a polar angle region between 11° and 169°. The track selection imposes additional constraints, selecting charged tracks only if :

- their momentum is between 0.1 GeV and $1.5 \cdot E_{\mathsf{beam}}$,
- the relative error on the momentum measurement is less than 100%,
- the distance of their closest approach to the beam-spot is less than 4 cm in the plane perpendicular to the beam axis and less than $4/\sin\theta$ cm along the beam axis.

For jet clustering and the computation of event cut variables, neutral particles are also used. They are accepted in a polar angle region between 3° and 177°, which gives a good rejection of off-momentum electrons. A minimum energy cut is applied on neutral tracks, which is 0.3 GeV for the barrel electromagnetic and small angle calorimeters, HPC and STIC, and 0.4 GeV for the electromagnetic calorimeter in the forward region, FEMC.

3 Event Selection

The signal coming from the process $e^+e^- \to qq(\gamma)$ was selected using global event variables deduced from the set of selected tracks. The following set of cuts provides a selection of hadronic events while rejecting Bhabha and two-photon background events:

- $N_{\mathsf{charged}} \geq 7$,

- $E_{\mathsf{FEMC}} := \sqrt{E_{\mathsf{F}}^2 + E_{\mathsf{B}}^2} \leq 85\%\, E_{\mathsf{beam}}$,
- $\sum E_{\perp} \geq 20\%\, E_{\mathsf{CMS}}$,
- $E_{\mathsf{charged}} \geq 10\%\, E_{\mathsf{CMS}}$.

E_{FEMC} is constructed from E_{F} and E_{B}, the sum of all showers found in the forward and backward arms of the forward electromagnetic calorimeter. Cutting on this quantity as a percentage of the beam energy rejects electrons from bhabha events. The request for a minimum transverse energy, $\sum E_{\perp}$, rejects two-photon events better than a comparably high E_{charged} cut, thus allowing the latter to be reduced.

At energies well above the Z-resonance, not only two-fermion final states with an effective centre-of-mass energy $\sqrt{s'}$ near the initial energy $\sqrt{s}$ contribute to the sample of measured events, but also radiative return events with $\sqrt{s'} \sim m_Z$ and several kinds of four-fermion events. To be able to study the values of R_b at $\sqrt{s'} \sim \sqrt{s}$, additional selection criteria are applied:

- Four-fermion events coming from the process $e^+e^- \rightarrow WW/ZZ \rightarrow qqqq$ usually can be easily forced into a four-jet structure and lead to a high $(1-T)$ value. Two-fermion events with a back-to-back topology have, if forced into four jets as well, at least one jet with considerably lower energy and smaller angle towards a neighbouring jet. An energy-dependent cut on $E_{\mathsf{min}} \cdot \Theta_{\mathsf{min}}$ and a remaining soft cut on the Thrust, $(1-T) \leq 0.31$ (0.35 for 1997,1998), further reduce the contamination with four-fermion events. An $E_{\mathsf{min}} \cdot \Theta_{\mathsf{min}} \leq \sqrt{s} \cdot 0.083^\circ$ cut is chosen for the data of 1997, $E_{\mathsf{min}} \cdot \Theta_{\mathsf{min}} \leq \sqrt{s} \cdot 0.079^\circ$ for 1998 and $E_{\mathsf{min}} \cdot \Theta_{\mathsf{min}} \leq \sqrt{s} \cdot 0.075^\circ$ for 1999 and 2000.
- The acceptance is limited to the silicon tracker polar angle coverage by requiring the thrust axis to have a minimal polar angle of 25°.
- The high energy sample is defined by rejecting any event with a reconstructed centre-of-mass energy $\sqrt{s'}$ [3] lower than 85% of the initial centre-of-mass energy.

Furthermore, runs which do not fulfill the demands on the detector quality were rejected, along with very short fills, where the beamspot was not reliably reconstructed and the b tagging degraded.

The influence of remaining background events was estimated using full detector simulation data sets generated by the EXCALIBUR four-fermion generator in versions 0.91, 1.01, 1.08 and 2.01 for different years of data taking. High energy and radiative $q\bar{q}(\gamma)$ events were simulated using the PYTHIA generator, versions 5.72 and 6.125.

The data sets analysed and the number of selected events obtained via the above selection cuts are listed in table 1.

4 Problems During the 2000 Data Taking

During the last third of data-taking in 2000 one twelfth of the main tracking detector TPC was missing due to a short between sense wires. As a consequence, although tracks in that angular region could still be reconstructed from hits in other tracking devices, the track finding efficiency and track resolution went down in that sector [4]. Special

$\sqrt{s}$	$\int \mathcal{L}\, dt$	$N_{\mathrm{had}}^{\mathrm{RD}}$
182.65	53.20(8)	1428
188.63	157.5(2)	3642
191.58	25.11(7)	551
195.52	76.1(2)	1640
199.52	83.0(2)	1633
201.64	40.0(1)	792
204.85	81.4(2)	1565
206.54	133.4(2)	2593

Table 1: Average energies, integrated luminosities and numbers of selected hadronic events for the analysed data sets

simulation was generated for that period, which started on the 1st of September and comprises $55.6\,\mathrm{pb}^{-1}$. An extra sample of Z pole data was taken so that the same analysis chain could be run separately on the data before and after the loss of the chamber, using the corresponding Z^o calibration runs and simulation data.

For the R_b and A_{FB}^b analyses the relevant distributions have been studied on both data sets separately, and no significant deterioration could be found in the agreement between data and simulation. Dedicated control plots such as the agreement in the number of b-jets reconstructed per sector show that the drop in efficiency is well described by simulation. The dilution factor needed to extract A_{FB}^b (see section 7) was degraded by about 4%, again with good agreement between data and simulation.

5 Identification of b Quarks

The DELPHI silicon tracker [5] provides up to six three dimensional points per track from three layers at radii between 6 and 11 cm. The precise track extrapolations provide a means of distinguishing between tracks from the primary vertex and tracks coming from decays of short lived hadrons.

The characteristics of heavy quark production are expressed in three observables:

- a lifetime variable constructed from the impact parameters in a jet,
- the mass of the secondary vertex if one is present.
- the rapidities of the tracks from the secondary vertex or jet.

These variables are combined in an event probability variable ranging from -5 to +10. A detailed description of the observables and their combination can be found in [6].

High values of the tagging variable correspond to a high b purity, whereas light quark events are accumulated at low values. $c\bar{c}$ events are enriched in the intermediate region but

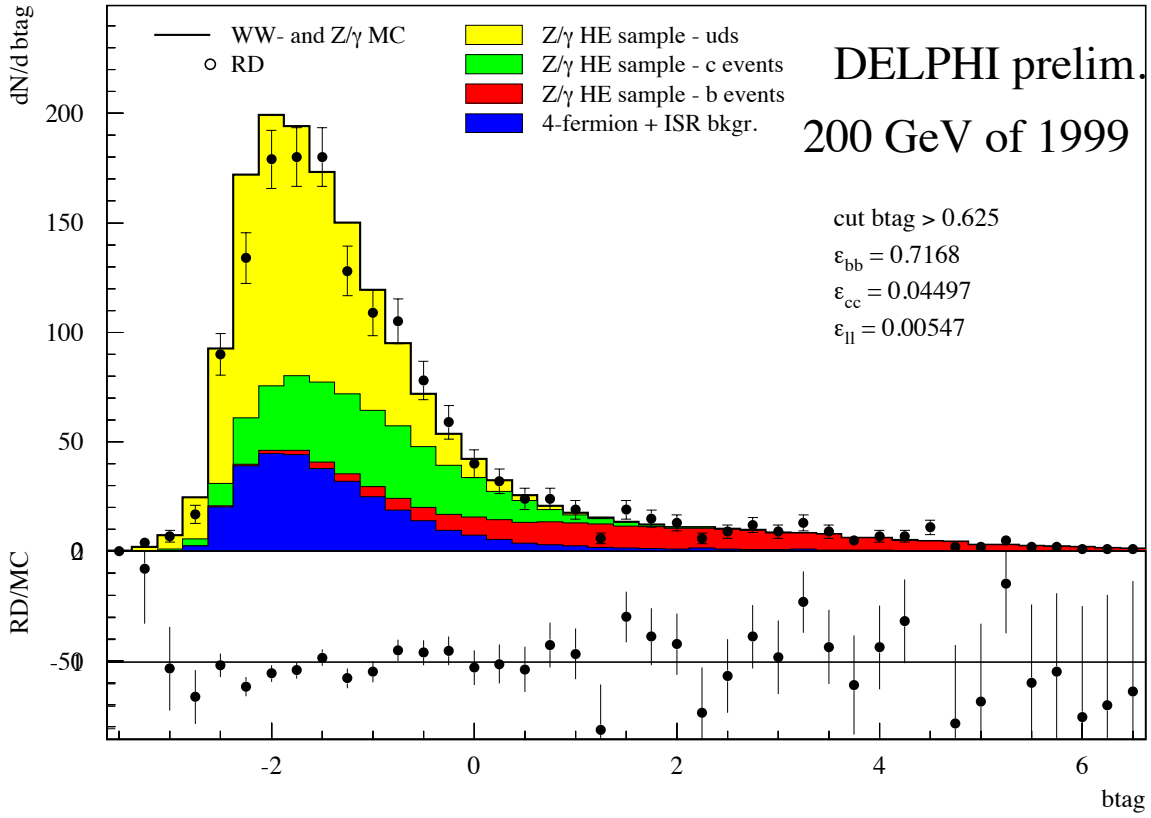

Figure 1: Distribution of the event tagging variable in the 200 GeV data set. The simulation is divided into $b\bar{b}$, $c\bar{c}$, light quark and background events. The quality of the agreement between data and simulation is an ingredient of the systematic error estimation.

are not clearly separated from the other flavour types. The distribution of the probability variable is displayed in figure 1 for the selected events measured at $\sqrt{s} = 200\,\mathrm{GeV}$ together with the simulation prediction consisting of Z/γ^* signal and different background types.

6 The R_b Measurement

By cutting on the event probability variable at $\mathcal{P}_b > 0.625$, a subsample ($N^{\mathsf{RD}}_{\mathsf{tagged}}$) is selected from the total number of selected events ($N^{\mathsf{RD}}_{\mathsf{total}}$) with a b purity between 88% and 90%, depending on the data set. When the background content is subtracted from the tagged and total selected events, the ratio of the two numbers can be expressed as a function of R_b using the tagging efficiencies for b, c and uds quarks (ε_b, ε_c, ε_{uds}).

$$\frac{N^{\mathsf{RD}}_{\mathsf{tagged}} - N^{\mathsf{ISR}}_{\mathsf{tagged}} - N^{\mathsf{4f}}_{\mathsf{tagged}}}{N^{\mathsf{RD}}_{\mathsf{total}} - N^{\mathsf{ISR}}_{\mathsf{total}} - N^{\mathsf{4f}}_{\mathsf{total}}} = R_b\,\varepsilon_b^{\mathsf{meas.}} + R_c^{\mathsf{SM}}\,\varepsilon_c^{\mathsf{MC}} + (1 - R_b - R_c^{\mathsf{SM}})\,\varepsilon_{uds}^{\mathsf{MC}} \qquad (1)$$

The constraint that the cross section ratios add up to one requires that R_{uds} contains the measured R_b as well. The different coefficients are explained more detailed in the

following.

6.1 Background estimation

The event selection reduces the remaining radiative return contamination to $\sim 8\%$ and four-fermion background to $\sim 18\%$, with the latter dropping to 3% in the WW-depleted b tagged sample.

The remaining backgrounds from selected four-fermion events ($N^{\mathsf{4f}}_{\mathsf{tagged}}$, $N^{\mathsf{4f}}_{\mathsf{total}}$) and from radiative events ($N^{\mathsf{ISR}}_{\mathsf{tagged}}$, $N^{\mathsf{ISR}}_{\mathsf{total}}$) contribute to the samples of selected and tagged events. They are estimated to be

$$N^{\mathsf{4f,\,ISR}}_{\mathsf{tot/tag}} = \left(\int \mathcal{L}\right) \cdot \sigma_{\mathsf{4f},\,Z/\gamma*} \cdot \varepsilon^{\mathsf{4f\,ISR}}_{\mathsf{tot/tag}} \tag{2}$$

and then subtracted from the number of measured events.

The cross section for four-fermion background (σ_{4f}) was taken from the Monte Carlo generator, EXCALIBUR, whereas the $q\bar{q}(\gamma)$ cross section ($\sigma_{Z/\gamma*}$) is replaced by the semi-analytic ZFITTER [9] prediction. As ZFITTER and PYTHIA agree very well in the distribution of the true $\sqrt{s'}$, the fraction of radiative two-fermion events is taken from simulation. It is contained in $\varepsilon^{\mathsf{ISR,4f}}$, which is in both cases defined as the ratio of selected events to all events found in the simulated data set. Table 2 shows the resulting estimated background contamination compared to the number of events in the data sample for the 200 GeV measurement.

	real data	ISR bg	4f bg
N_{total}	1633	102(2)	285(2)
N_{tagged}	206	14.3(5)	8.1(3)

Table 2: Example of N^{ISR}, N^{4f} estimated based on eq. 2 for the 200 GeV data sample. The errors are related to the limited simulation statistics.

6.2 Efficiency determination

In order to minimise the dependence on the description of the b-modelling in the simulation, the b efficiency ε_b is calibrated by applying equation 1 to the Z peak data of the corresponding LEP running period. The accurately measured cross section ratio from the LEP 1 period is used [7], leading to a measured ε_b^0 which is then extrapolated to high energies. Thus only the relative change in efficiency needs to be taken from simulation. More precisely, the inefficiency $\bar{\varepsilon}$ is extrapolated, giving

$$\varepsilon_b^{\mathsf{meas.}} = 1 - r \cdot (1 - \varepsilon_b^0) \text{ with the relative change } r = \frac{\bar{\varepsilon}^{\mathsf{MC}}(E)}{\bar{\varepsilon}^{\mathsf{MC}}(m_Z)}. \tag{3}$$

ε_c and ε_{uds} are taken directly from high energy simulation.

6.3 R_c and acceptance correction

Standard Model predictions for R_c at high energies as well as on the peak are obtained from ZFITTER[2] [9].

The Standard Model ratios measured at LEP 1 and predicted by ZFITTER correspond to the full angular acceptance and a 100% hadronic selection efficiency. The Standard Model ratios are acceptance corrected before they are used in eq. 1. The measured R_b results are corrected to full acceptance.

6.4 Sources of systematic error

The following sources of systematic error are taken into account:

- Systematic errors can arise from uncertainties in the flavour tagging method, from the stability of the b tagging for different data taking periods and the way the detector resolution enters the tagging.

  They are determined by swapping the b tagging calibration files for real data and simulation and by shifting the probability variable distributions for c and uds events to higher values, improving the agreement in the probability distribution on the Z. The second change is smaller than the first due to the high purity working point, away from the region where disagreements are generally observed.

  For the 2000 data the detector alignment and consequently the b tagging calibration still shows problems with the current, not yet final data processing. The systematic error arising from this was estimated by switching between different b tagging calibrations from different data-taking periods. The result is that the preliminary systematic error given for detector and b tagging is about half the statistical error. It was assumed fully correlated while combining the results from the periods before and after the TPC sector loss.

- Imperfections in the b modelling do not enter the analysis method directly, because it calibrates itself on the Z data. However the statistical errors of the Z data sets, and also of the simulated samples used for extrapolation, result in an uncertainty in ε_b, which is of the same order of magnitude as the difference between calibrated and simulated ε_b. The corresponding effect on R_b is quoted as ε_b uncertainty.

- Uncertainties in the c and uds modelling have been studied for the LEP 1 R_b measurement [7]. They arise mainly from the $c\bar{c} \to D^+$ fraction and the D decay multiplicity in case of ε_c, and from light hadron modelling and gluon splitting in case of ε_{uds}. Their size is scaled to the working point of this analysis and multiplied with a confidence factor of 2, taking into account the different working point and energy.

- Another source of systematic error originates from correcting the measured R_b to full acceptance. Its size is taken as one third of the correction.

- For the four-fermion background modelling, it has to be taken into account that very small contributions such as Zee and $llqq$ events have been neglected, and that the

[2]Version 6.22 with the `FINR` flag set to 0

Energy [GeV]	**182.65**	**188.63**	**191.58**	**195.52**	**199.52**	**201.64**	**204.85**	**206.54**
stat error MC	0.0006	0.0006	0.0022	0.0008	0.0008	0.0013	0.0008	0.0007
ε_b error	0.0023	0.0020	0.0033	0.0019	0.0020	0.0024	0.0047	0.0043
accept. corr.	0.0005	0.0007	0.0001	0.0004	0.0009	0.0009	0.0011	0.0008
4f BG modelling	0.0010	0.0013	0.0015	0.0015	0.0020	0.0019	0.0019	0.0017
ε_c uncertainty	−0.0019	−0.0023	−0.0022	−0.0024	−0.0024	−0.0025	−0.0020	−0.0021
ε_{uds} uncertainty	−0.0012	−0.0013	−0.0013	−0.0012	−0.0014	−0.0013	−0.0010	−0.0013
detector resolution	0.0018	0.0012	0.0015	0.0016	0.0016	0.0016	0.0088	0.0085
$\sqrt{s'}$ cut var.	−0.0008	−0.0005	−0.0013	−0.0007	−0.0008	−0.0011	−0.0009	−0.0009
INTF modelling	0.0009	0.0009	0.0009	0.0009	0.0009	0.0009	0.0009	0.0009
total	**0.0041**	**0.0040**	**0.0055**	**0.0043**	**0.0047**	**0.0050**	**0.0106**	**0.0101**
(stat. error RD)	0.0154	0.0103	0.0262	0.0150	0.0160	0.0229	0.0164	0.0120
R_c dependence (α)	−0.0473	−0.0557	−0.0540	−0.0594	−0.0581	−0.0617	−0.0484	−0.0492

Table 3: List of systematic uncertainties. A negative sign denotes an anti-correlation with respect to variation. The total systematic error is computed as quadratic sum of all preceding contributions.

Energy [GeV]	R_b ($\pm$stat, $\pm$syst. error)	SM expectation
182.65	$0.1373 \pm 0.0154 \pm 0.0041$	0.1671
188.63	$0.1563 \pm 0.0103 \pm 0.0040$	0.1660
191.58	$0.1688 \pm 0.0262 \pm 0.0055$	0.1655
195.52	$0.1653 \pm 0.0150 \pm 0.0043$	0.1648
199.52	$0.1834 \pm 0.0160 \pm 0.0047$	0.1642
201.64	$0.1775 \pm 0.0229 \pm 0.0050$	0.1639
204.85	$0.1668 \pm 0.0164 \pm 0.0106$	0.1634
206.54	$0.1567 \pm 0.0120 \pm 0.0101$	0.1632

Table 4: Preliminary results for R_b at energies between 183 and 207 GeV. Statistical and systematic errors are quoted separately. The Standard Model prediction has been computed with ZFITTER.

estimation relies on the correct knowledge of cross sections and data luminosities. These effects are summarised in a variation of the four-fermion cross section by $\pm 5\%$, which is larger than its theoretical error ($2-3\,\%$).

- The cut on the reconstructed centre-of-mass energy could introduce a bias due to ISR modelling or detector effects. Its size is estimated by varying the cut by $\pm 5\,\%$ and averaging the impact on R_b over all 6 energy points in order to minimise the influence of statistical fluctuations. A cross check is performed by going back to a simpler form of the $\sqrt{s'}$ reconstruction algorithm which uses only topological information. Its effect is in agreement with the cut variation.

- A theoretical uncertainty in the modelling of the initial state / final state QED interference is quoted as well ("INTF modelling"). It is taken as half the change in the ZFITTER prediction when switching off the $\mathcal{O}(\alpha)$ interference correction, which is active by default.

An overview of the individual systematic error contributions for each of the six energy points is given in table 3. The total systematic error on R_b is obtained by quadratic summation and can be compared to the statistical error on real data.

The dependence on R_c is quoted in the systematic error breakdown in table 3 as well; it refers to the proportionality factor between R_b and the deviation from the Standard Model expectation: $R_b = R_b^{\mathsf{meas.}} + \alpha \cdot (R_c - R_c^{\mathsf{SM}})$.

6.5 Results

The measured results for R_b are summarised in table 4 and plotted in figure 2 together with the prediction from ZFITTER. The plot also contains published measurements both on-peak and off-peak [7] and the 130-172 GeV results from [2]. Both the high energy ($\sqrt{s'}/\sqrt{s} > 0.85$) and the inclusive ($\sqrt{s'}/\sqrt{s} > 0.10$) theoretical prediction are included

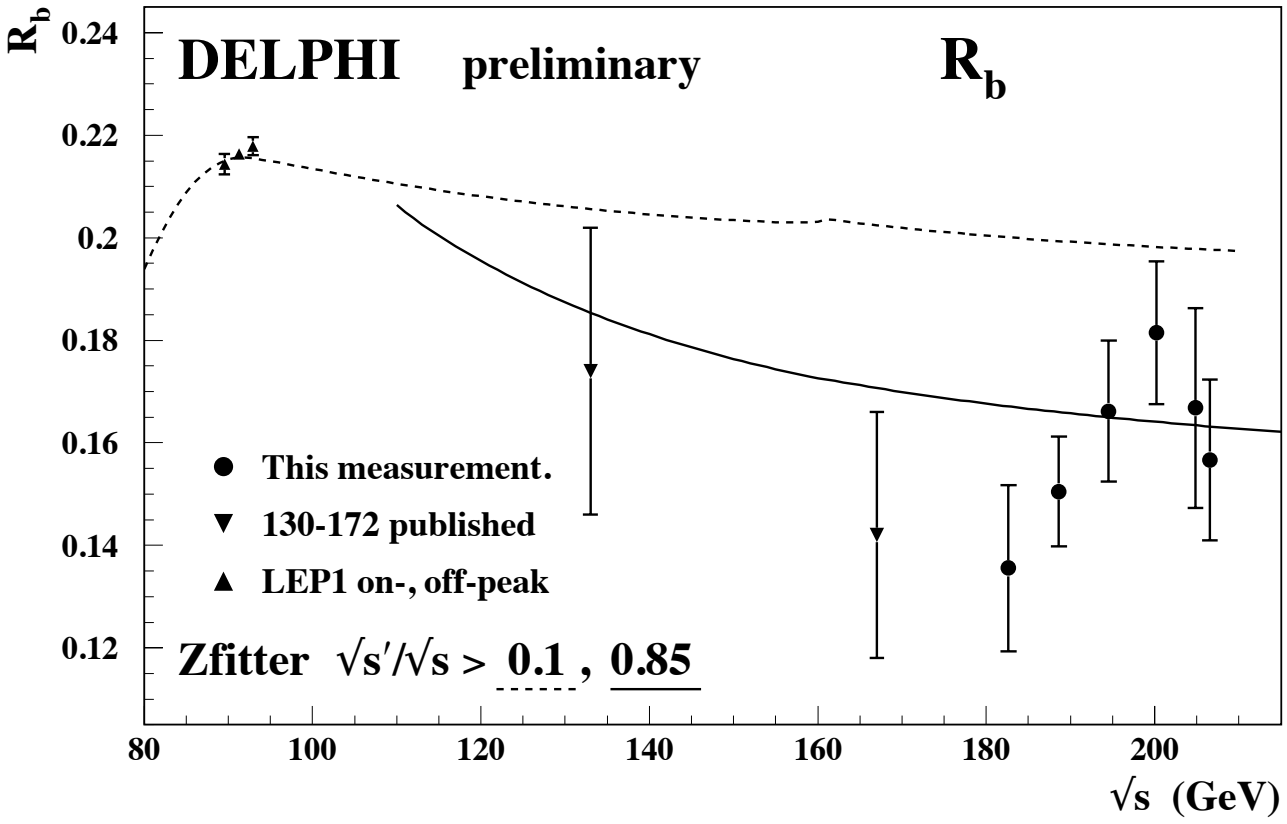

Figure 2: The cross section ratio R_b versus the LEP centre-of-mass energy $\sqrt{s}$. The data points show the preliminary results obtained with this analysis (closed circles) and previous results published in [2] and [7]. The LEP 2 results have to be compared with the high energy prediction ($\sqrt{s'}/\sqrt{s} > 0.85$) given by ZFITTER (full curve). In this plot the 192 and 196 GeV and the 200 and 202 GeV measurements have been combined.

in the plot. The measured R_b values show a good agreement with the Standard Model within their statistical errors.

7 The A_{FB}^b Measurement

For events with a reconstructed centre-of-mass energy $\sqrt{s'}$ of close to 200 GeV, the forward-backward asymmetries, A_{FB}, of quarks are expected to be significantly higher than at the Z pole. The angular distribution of the b quarks as a function of their production angle θ can be described by

$$\frac{d\sigma}{d\cos\theta} = 1 + \cos^2\theta + \frac{8}{3}A_{FB}\cos\theta, \tag{4}$$

where uncertainties due to the interference between initial and final state radiation have been neglected, as their impact on the measurement described here is small [11].

Experimentally the quark charge can be estimated from the final state particles. In the regime $\sqrt{s'}/\sqrt{s} > 0.85$ the events are back-to-back, and the thrust axis of the event may be used to divide the event into forward and backward hemispheres, where the forward hemisphere is defined to be the one containing the incoming electron. The momenta of the charged tracks are projected onto the forward unit thrust axis $\overrightarrow{T}$, and the charges of the forward (Q_F) and backward (Q_B) hemisphere are computed to be:

$$\mathrm{Q_{F(B)}} = \frac{\sum_i q_i |\overrightarrow{p}_i \cdot \overrightarrow{T}|^\kappa}{\sum_i |\overrightarrow{p}_i \cdot \overrightarrow{T}|^\kappa} \tag{5}$$

where q_i is the particle charge, p_i its momentum, and the exponent κ is set to a value of 0.6, chosen to optimise the discrimination. The sum runs over all charged tracks i, and all terms with $\overrightarrow{p}_i \cdot \overrightarrow{T} > 0$ contribute to Q_F, while all terms with $\overrightarrow{p}_i \cdot \overrightarrow{T} < 0$ contribute to Q_B. The information from the two hemispheres is combined in the charge flow variable Q_{FB},

$$Q_{FB} = Q_F - Q_B \tag{6}$$

the sign of which is sensitive to whether the b quark is in the forward or backward hemisphere. The knowledge of the true quark charge is limited by the fragmentation, but improves for greater absolute values of Q_{FB}. If a cut is made requiring $|Q_{FB}| > 0.1$ the fraction of b events with an incorrect charge assignment, ω_q, is about 0.26 according to the Monte Carlo.

The variable x is defined to be the cosine of the event thrust axis signed by $-Q_{FB}$. The observed asymmetry A_{FB}^{obs} is fitted to the distribution of the events in x by maximising the likelihood

$$\ln \mathcal{L} = \sum_i \ln\,(1 + x_i^2 + \frac{8}{3}A_{FB}^{obs}x_i) \tag{7}$$

where the sum runs over all events. The observed charge asymmetry contains contributions from the various backgrounds included in the sample. The WW background and the contamination from low $\sqrt{s'}$ are subtracted with asymmetries as measured on the Monte Carlo, giving corrections of about 3%. The remaining asymmetry can be expressed as

$$A_{FB}^{obs} = \sum_{q=u,d,s,c,b} s_q D_q A_{FB}^q F_q \tag{8}$$

where the sum is over the quark species, A_{FB} is the asymmetry, F the relative abundance, D a dilution factor for each quark coming from charge misassignment, and the sign s is $+1$ for b, d and s quarks, and -1 for u and c quarks. The dilution factors are determined from the Monte Carlo, by repeating the maximum likelihood fit on the Monte Carlo sample with and without use of the truth information to determine Q_{FB}. For the quarks other than the b quarks the Standard Model value for A_{FB}^q is taken. For this analysis, a high-purity working point is chosen with $F_b = 0.96$ and $F_c = 0.03$, minimising the corrections due to the non b quark contamination. This formula is used to extract A_{FB}^b.

The fit to the distribution in the variable x is illustrated in figure 3 for the data sets from 189 to 202 GeV.

7.1 Systematic Error Estimation

The principal contributions to the systematic error were as follows:

- **Knowledge of the dilution factors**. The dilution factors were cross checked using the values of ω_q as measured on the Monte Carlo, and the relation $D_q = 1 - 2\omega_q$. The knowledge of the dilution factors was also checked by making the measurement on the Z^0 data accumulated in 1998, 1999 and 2000 and comparing to the LEP1 measured value of A_{FB}^b, and by looking at variations between the different years and energy points. Finally the exponent κ was varied between values of 0.3 and 0.9 and the dilution factors recomputed. The systematic error estimated from the variations between these methods was 7%.

- **Detector Effects.** The following detector effects were considered:

  - Variation of purity with $\cos\theta$
  - Changes of beamspot size and width between years and data samples
  - Estimated asymmetry in detector efficiency
  - Placement in z of the silicon tracker in data and simulation

  A conservative error from these effects was estimated to be 5%.

- **Backgrounds.** The WW and ISR backgrounds were varied by 50%, leading to an uncertainty of less than 2%.

- **2000 TPC problems.** The data from the period with TPC problems was investigated separately. It was shown that the fluctuations seen with the problem sector removed lay well within those seen when removing an arbitrary sector.

The total systematic error was estimated at 9%. Note that the chosen working point means that the dependence of the result on the assumed branching fractions into $b\overline{b}$ and $c\overline{c}$ is negligible.

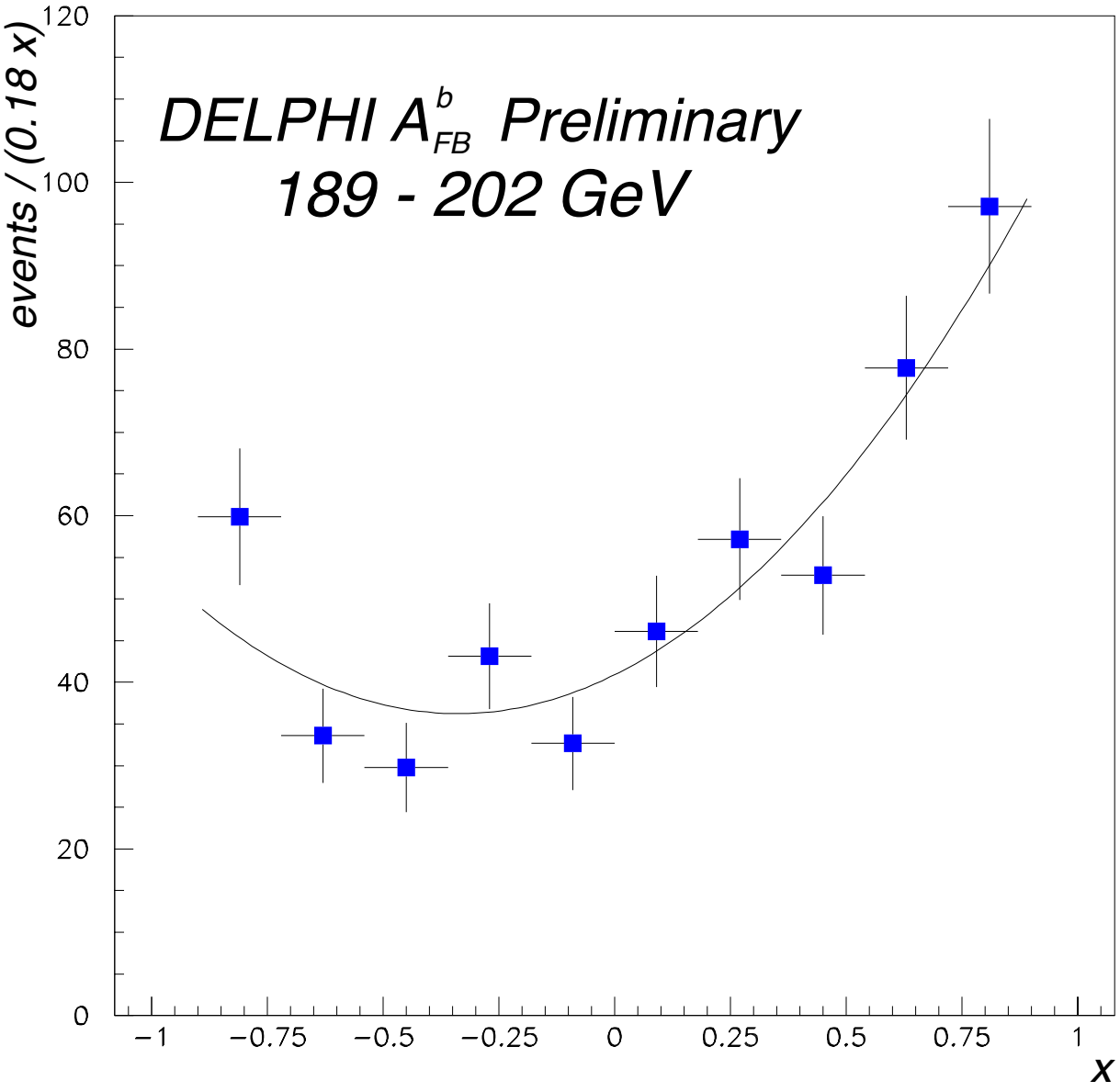

Figure 3: The distribution of the variable x, the signed $\cos\theta$ of the event thrust axis, for the data sets from 189 GeV to 202 GeV inclusive. The data points have a symmetric $\cos\theta$ correction applied for the b tagging efficiency. The line shows the result of the maximum likelihood fit to A_{FB}^{obs}.

Energy (GeV)	number of selected events	$A^b_{FB} \pm$ stat. $\pm$ syst. error
188.6	206	$0.50^{+0.13}_{-0.14} \pm 0.05$
191.6	44	$0.37^{+0.30}_{-0.31} \pm 0.03$
195.5	110	$0.72^{+0.18}_{-0.19} \pm 0.06$
199.5	117	$0.74^{+0.18}_{-0.19} \pm 0.07$
201.6	53	$0.59^{+0.27}_{-0.29} \pm 0.05$
204.8	79	$0.76 \pm 0.25 \pm 0.07$
206.6	157	$0.47 \pm 0.20 \pm 0.08$

Table 5: Preliminary results for A^b_{FB} at energies between 189 and 207 GeV. Statistical and systematic errors are quoted separately.

7.2 Results

The measured results for A^b_{FB} are summarised in table 5 and plotted in figure 4 together with the prediction from ZFITTER, and the previously published values. The measurements are compatible with the Standard Model predictions.

8 Interpretation

Deviations from the Standard Model predictions for the process $e^+e^- \to b\bar{b}$ can be described model-independently in form of effective four-fermion contact interactions, giving access to new physics at higher energy scales. The heavy flavour production results have been used to obtain limits on such contact interaction scales.

Contact interactions are parametrised by an effective Lagrangian [12] of the form

$$\mathcal{L}_{\text{eff}} = \frac{g^2}{\Lambda^2} \sum_{i,j=L,R} \eta_{ij} (\bar{e}_i \gamma_\mu e_i)(\bar{f}_j \gamma^\mu f_j) \qquad , \quad f \neq e, \tag{9}$$

where e_i and f_j denote left or right-handed spinors and the coupling $g^2/4\pi$ is taken to be 1 by convention. Different helicity couplings $\eta_{ij} = \pm 1$ or 0 between initial and final state fermions can be assumed, defining a set of different models [13]. Each can have constructive (+) or destructive (−) interference with the Standard Model Lagrangian. Only the models explained in table 6 have been studied since they lead to large deviations in the $e^+e^- \to b\bar{b}$ production.

All R_b and A^b_{FB} results above the Z^o resonance are used as inputs, i.e. for 133 GeV, 167 GeV from [2] and for 183 (189 in case of A^b_{FB}) to 207 GeV from tables 4 and 5. Hereby the R_b measurement has to be converted into a cross-section $\sigma_{b\bar{b}}$ using the DELPHI hadronic cross section measurements published in [14]. The method of fitting each contact interaction model to the data works by fitting a parameter ϵ defined as $\epsilon = 1/\Lambda^2$. This parameter can take both positive and negative values in the fit and is 0 in the limit that no contact interactions exist. In the calculation of errors correlations between R_b and $\sigma_{b\bar{b}}$

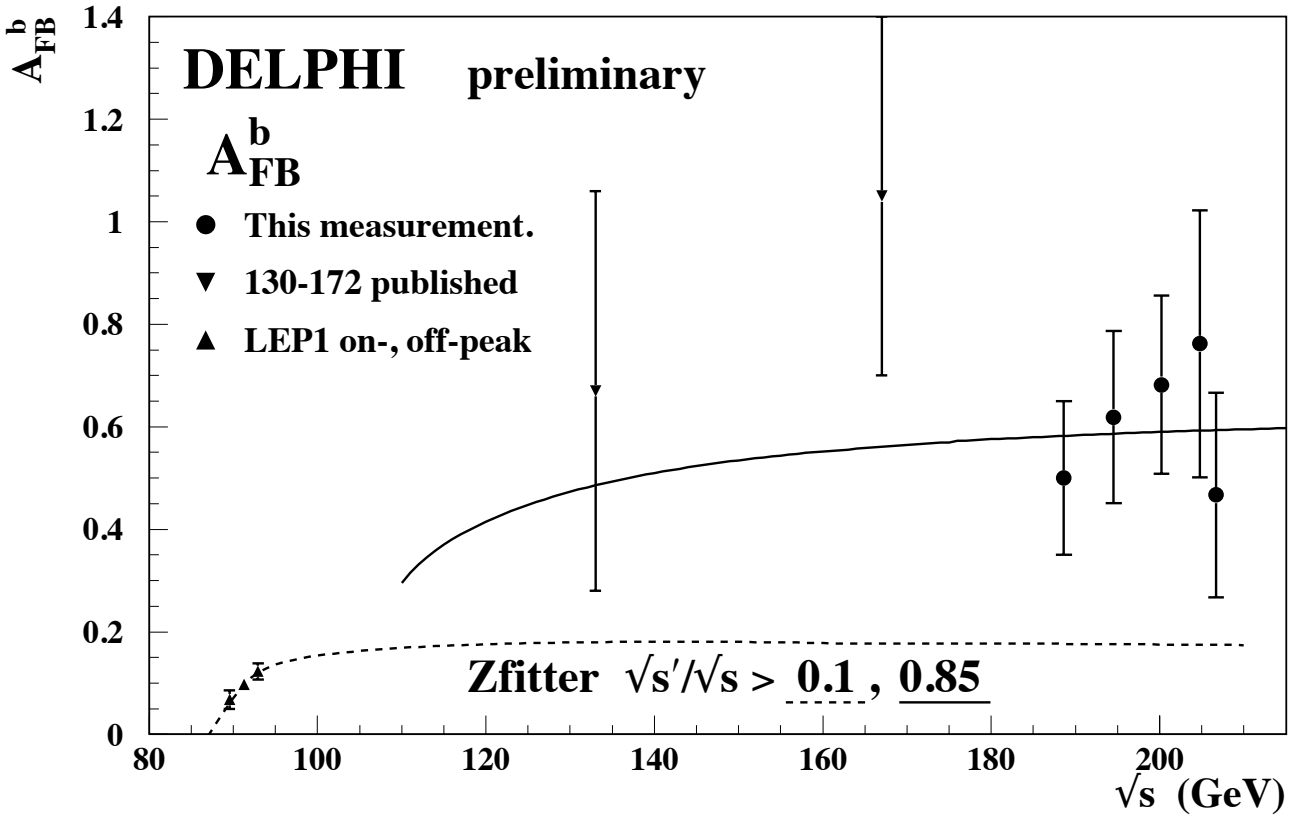

Figure 4: The b quark asymmetries A_{FB}^b versus the LEP centre-of-mass energy $\sqrt{s}$. The data points show the preliminary results obtained with this analysis (closed circles) and previous results published in [2] and [10]. The solid line shows the high energy prediction ($\sqrt{s'}/\sqrt{s} > 0.85$) given by ZFITTER.
Like the R_b results, the 192 and 196 GeV and the 200 and 202 GeV measurements have been combined.

Model	η_{LL}	η_{RR}	η_{LR}	η_{RL}
$LL^{\pm}$	±1	0	0	0
$RR^{\pm}$	0	±1	0	0
$VV^{\pm}$	±1	±1	±1	±1
$AA^{\pm}$	±1	±1	∓1	∓1
$LR^{\pm}$	0	0	±1	0
$RL^{\pm}$	0	0	0	±1
$V0^{\pm}$	±1	±1	0	0
$A0^{\pm}$	0	0	±1	±1

Table 6: Choices of η_{ij} for different contact interaction models

.

$e^+e^- \to b\bar{b}$			
Model	ϵ (TeV^{-2})	Λ^- (TeV)	Λ^+ (TeV)
LL	$-0.0006^{+0.0074}_{-0.0078}$	7.9	8.4
RR	$-0.1626^{+0.1610}_{-0.0350}$	2.2	5.7
VV	$-0.0005^{+0.0041}_{-0.0043}$	8.6	9.5
AA	$-0.0006^{+0.0032}_{-0.0034}$	9.6	10.7
RL	$0.0459^{+0.1299}_{-0.0201}$	3.0	4.7
LR	$0.1274^{+0.0330}_{-0.1217}$	5.8	2.4
V0	$-0.0004^{+0.0053}_{-0.0056}$	9.3	9.9
A0	$0.0313^{+0.0272}_{-0.0381}$	5.4	3.7

Table 7: Fitted values of ϵ and 95% confidence limits on the scale, Λ, for constructive (+) and destructive interference (−) with the Standard Model, for the contact interaction models discussed in the text. From $b\bar{b}$ results with centre of mass energies from 133 to 207 GeV.

were assumed negligible. However correlations between different energy points were taken into account by the fit.

The results for ϵ for each of the models are shown in table 7 together with their 68% confidence level uncertainty. They are all compatible with the Standard Model expectation of $\epsilon = 0$. The lower limits on Λ are obtained by integrating the likelihood function over the physically allowed values, $\epsilon \geq 0$ for each Λ^+ limit and $\epsilon \leq 0$ for Λ^- limits. The resulting limits for a 95% confidence level are also shown in table 7 and are displayed in figure 5.

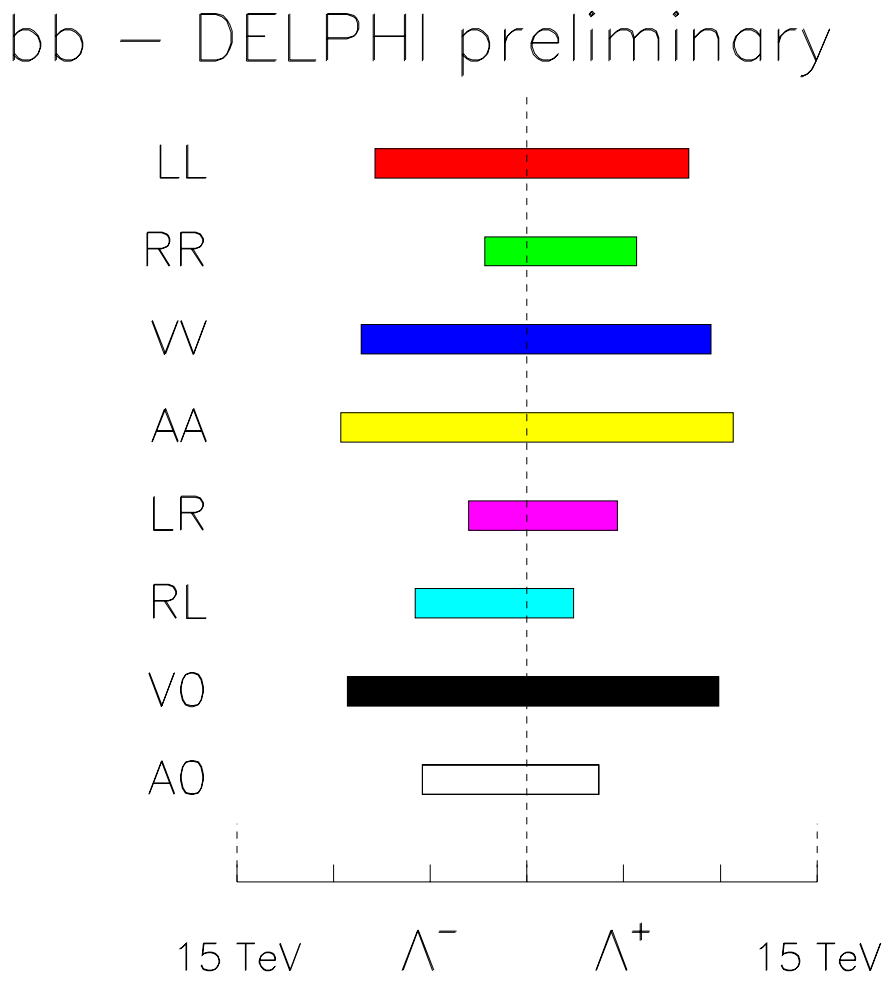

Figure 5: Graphical display of the excluded values for the scale Λ for each model (95% CL). Positive (negative) values denote constructive (destructive) interference with the Standard Model.

References

[1] DELPHI Coll. – P.Abreu et al., Nucl. Inst. and Meth. **A** 378 (1996) 57.

[2] DELPHI Coll. – P.Abreu et al., Eur. Phys. J. **C11** (1999) 383.

[3] P. Abreu et al., *SPRIME – A Package for Estimating the Effective $\sqrt{s'}$ Centre of Mass Energy in $q\bar{q}\gamma$ Events*, DELPHI internal note 96-124 PHYS 632;
P. Abreu et al., *The Estimation of the Effective Centre of Mass Energy in $q\bar{q}\gamma$ Events from DELPHI*, unpublished.

[4] M. Elsing et al., *Changes in the track reconstruction to recover from the TPC sector 6 failure*, DELPHI internal note 2001-004 TRACK 95

[5] The DELPHI Silicon Tracker Group – P. Chochula et al., Nucl. Inst. Meth **A** 412 (1998) 304.

[6] G.V.Borisov, *Lifetime Tag of events $Z \to b\bar{b}$ with the DELPHI detector — AABTAG program*, DELPHI internal note 94-125 PROG 208;
G.V.Borisov, *Combined b tagging*, DELPHI internal note 97-094 PHYS 716.

[7] DELPHI Coll. – P.Abreu et al., Eur. Phys. J. **C10** (1999) 415.

[8] The LEP Collaborations et al., *A Combination of Preliminary Electroweak Measurements and Constraints on the Standard Model*, CERN-EP-2000-016.

[9] D. Bardin et al., *ZFITTER v.6.21 - A Semi-Analytical Program for Fermion Pair Production in e^+e^- Annihilation*, DESY 99-070 – hep-ph/9908433.

[10] DELPHI Coll. – P.Abreu et al., E. Phys. J. **C9** (1999) 367.

[11] ALEPH Coll., Phys. Lett. **B399** (1997) 329;
DELPHI Coll., Z. Phys. **C72** (1996) 31.

[12] E. Eichten, K. Lane and M. Peskin, Phys. Rev. Lett. **50** (1983) 811.

[13] H. Kroha, Phys. Rev. **D46** (1992) 58.

[14] DELPHI Coll. – P.Abreu et al., CERN-EP/2000-068
DELPHI Coll., Contributed Paper 647 to ICHEP 2000, DELPHI internal note 2000-128 CONF 427
A. Behrmann et al., *Results on Fermion-Pair Production at LEP running in 2000*, DELPHI internal note 2001-022 CONF 463